Development of Numerical Removal Model of Arsenic from Groundwater

Razzak, Abdur
Executive Engineer, Waste Management Division, Dhaka North City Corporation, Bangladesh

Jinno, Kenji
Emeritus Professor, Kyushu University

Hiroshiro, Yoshinari
Assoc. Professor, Department of Urban and Environmental Engineering

出版情報：九州大学工学紀要. 72 (3), pp.85-102, 2012-09-03. 九州大学大学院工学研究院
バージョン：
権利関係：

Memoirs of the Faculty of Engineering, Kyushu University, Vol. 72, No.3, September 2012

Development of Numerical Removal Model of Arsenic from Groundwater

by

Abdur RAZZAK*, Kenji JINNO** and Yoshinari HIROSHIRO***

(Received July 19, 2012)

Abstract

There is a tremendous demand for developing efficient methods for arsenic removal from drinking waters due to its severe toxicity effect on living beings. In order to predict an appropriate technique for arsenic removal from groundwater a numerical model that is able to describe the removal of arsenic and other background species from the groundwater considering chemical and biochemical processes has been developed in the present paper. Based on the adsorption/co-precipitation of arsenic with iron(III) hydroxides, the behavior of arsenic and iron under oxidation dominant environment including advection, dispersion, molecular diffusion and the microbially mediated chemical processes are also presented. The arsenic transport equation and the balance equations are solved numerically using the finite difference method and method of characteristics (MOC), subject to prescribed initial and boundary conditions are also presented. The kinetic sub model describes the heterotrophic metabolisms of several groups of microorganisms. Microbial growth is assumed to follow Monod type kinetics. The results of the removal simulation model demonstrated that availability of substrate (e.g. organic carbon), maximum growth rate, yield coefficient of bacteria, the precipitation rate of iron-hydroxide and the adsorption/precipitation rate of arsenic with iron hydroxide were important parameters which affected the removal of arsenic from groundwater. Among all the parameters organic carbon concentration proved as the most important.

Keywords: Arsenic removal, Oxidizing condition, Microorganism, Simulation model

1. Introduction

Groundwater is used for drinking water supply as well as for industrial and irrigation purpose almost everywhere in the world and usually constitutes water of higher quality than the surface water, since it is typically free from diseases causing microorganisms. However, groundwater contamination by organic and inorganic pollutants is a major public concern in many regions across the world [1)]. Among all the pollutants arsenic is considered as a high priority one. As the presence of arsenic species in drinking water, even in low concentrations, is a threat to human health, the World Health Organization (WHO) recommended the new maximum contaminant level (MCL) of arsenic in drinking water to 10 ppb from an earlier value 50 ppb [2)], while some developing country like Bangladesh has been permitted a maximum arsenic level 50 ppb (five times higher than WHO standards) in groundwater supplies for drinking purpose [3)]. Several studies have linked long-term exposure even to small concentrations of arsenic with cancer and cardiovascular, pulmonary, immunological, neurological and endocrine effects. As a consequence, arsenic is considered highly

* Executive Engineer, Waste Management Division, Dhaka North City Corporation, Bangladesh
** Emeritus Professor, Kyushu University, Japan
*** Assoc. Professor, Department of Urban and Environmental Engineering

toxic and there is a tremendous demand for developing efficient methods for arsenic removal from drinking waters [4-5] to help developing countries.

The distribution of arsenic species (As(III), As(V)) in natural waters is mainly dependent on redox potential and pH conditions [6]. Under oxidizing conditions such as those prevailing in surface waters, the predominant species is pentavalent arsenic, which is mainly present with the oxyanionic forms ($H_2AsO_4^-$). On the other hand, under mildly reducing conditions such as in groundwaters, As(III) is the thermodynamically stable form, which at pH values of most natural waters is present as non-ionic form of arsenious acid (H_3AsO_3) [7]. Thus, As(III) may interact in smaller extent with most solid surfaces, therefore, it is more difficult to be removed by the conventional treatment methods, such as adsorption, precipitation, etc. [6].

Several treatment technologies have been developed for the removal of arsenic from water streams, such as sorption and ion-exchange [8], precipitation [9], coagulation and floculation [9-10] reverse osmosis [11], membrane technologies [12], electrodialysis [13], biological processes [6] as well as lime softening [14], etc. Among them, co-precipitation/adsorption processes are commonly applied today to meet the current drinking water standards and show a good efficiency to cost ratio for higher arsenic concentrations. Most of these technologies are not sufficiently efficient enough for the removal of As(III); hence, they are mainly applied for the removal of As(V). Therefore, a pre-oxidation step is usually required to transform the trivalent (As(III)) form to the pentavalent (As(V)) one [15]. The oxidation of As(III) is usually carried out by the addition of chemical reagents such as ozone, hydrogen peroxide, chlorine, or potassium permanganate [6, 16-17]. Although these reagents are effective for the oxidation of trivalent arsenic, they may also cause several secondary problems, arising mainly by the presence of residuals or from byproducts formation, inducing simultaneously a significant increase to the operational costs of respective methods. In recent years attention has been given to biological arsenic removal as it may have potential as a cost effective solution. As an alternative to chemical oxidation, bacterially catalyzed As(III) oxidation can be applied. Several species of bacteria have been found to mediate this process [7, 18-19], although, to date, only a few studies applying the biological arsenic oxidation directly in continuous groundwater treatment have been reported [1, 6, 15, 19]. As(III) can be oxidized to As(V) by dissolved oxygen, and this reaction was found to be mediated by specific bacteria that are indigenous in groundwater sources, the so-called “iron oxidizing bacteria”. Iron exerts a strong influence on arsenic concentrations in groundwaters. The application of biological iron oxidation, results in the formation of insoluble products (iron oxides), which are subsequently removed from water by filtration [20]. Thus the arsenic removal method based on biological iron oxidation would be an ideal option in developing countries.

Recently, Katsoyiannis et al. (2002) [19] used fixed-bed upflow bioreactors for Arsenic (III) removal from groundwater. They specifically used iron oxidizing bacteria in their study. Arsenic was removed around 80%. This method was reported to be suitable for iron and manganese oxidation along with arsenic removal. Katsoyiannis and Zouboulis (2004) [6] conducted further studies with iron oxidizing bacteria for removing both arsenite and arsenate. The results indicated that both forms of arsenic could be efficiently removed by for the concentration range of interest in drinking water. In addition the oxidation of trivalent arsenic was found to be catalyzed by bacteria leading to an increased arsenic removal because trivalent arsenic cannot be efficiently sorbed to iron oxides. Zouboulis and Katsoyiannis (2005) [21] conducted X-ray photoelectron spectroscopy (XPS) analyses to obtain information for the mechanism of As(III) removal by arsenic oxidizing iron bacteria. Results indicated that As(III) was partially oxidized to As(V) which enabled high arsenic removal efficiency.

The current literature indicates that there are no studies that have been directed towards simulating the arsenic removal from groundwater, considering physical, chemical and bio-geochemical processes in porous media. All the previous studies on arsenic removal investigated experimentally. The main objective of this study is to develop a numerical model that is able to produce accurate simulations of arsenic removal from groundwater and other background species considering physical, chemical and biochemical processes.

2. Model Development

2.1 Conceptual model

The model developed in this study is based on the established arsenic removal mechanism from water stream considering both chemical and bio-geochemical reaction processes under oxidation environment. The model considered three different phases are: mobile pore water phase, immobile bio phase and solid matrix phase as shown in **Fig. 1** and **Fig. 2**. The model assumed that the microorganisms reside in an immobile bio phase. The bio phase is commonly called bio-film. All chemical reactions take place in mobile phase and all biochemical reactions take place inside the bio phase. The chemical reaction rate is very slow compare with biochemical reaction rate also assumed in this model. The volume of the bio phase is assumed to be constant in time and space and not coupled to microbial growth [22].

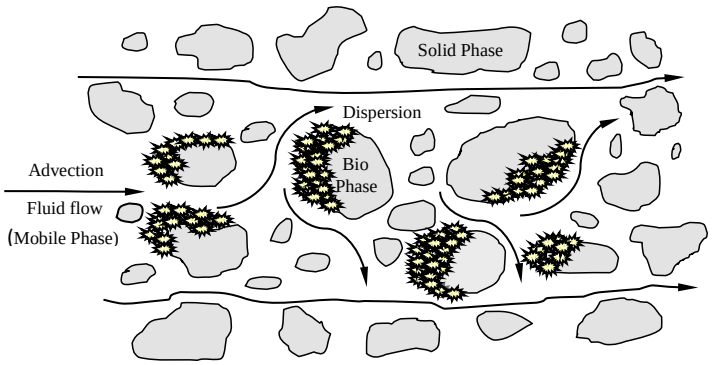

Fig. 1 Conceptual model of the processes occurring in a saturated porous media.

Oxygen is allowed to dissolve in the mobile phase as shown in **Fig. 2**. The organic compounds are assumed to be carried by the pore water or additionally supplied to the water. They can transfer to the bio phase, where their chemical composition changed by microbially mediated reactions such as oxidation. Other species involved in the microbial reactions such as electron acceptors reach the bio phase directly via the pore water (e.g., H_3AsO_3, Fe^{2+}). The metabolic products (e.g., $Fe(OH)_3$) directly goes to the matrix phase and further act as absorbent for another metabolic products like As(V) in the aquifer.

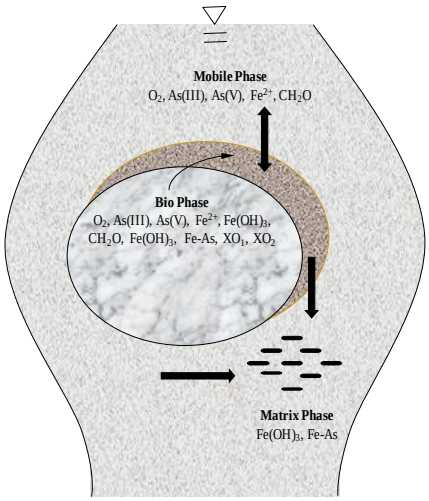

Fig. 2 Conceptual model of the aquifer phases, exchange relation, chemical and biochemical processes of different species residing in the phases.

Exchange processes are considered between the different phases, the mobile phase and the bio phase; the mobile phase and the matrix phase; and the bio phase and the matrix phase as shown in **Fig. 2**. The model also assumed two different species of bacteria (XO_1 and XO_2) are to grow in the bio phase.

2.2 Biochemical, chemical reactions and mathematical expression of bacteria growth

The modeling of complex redox sequences requires the consideration of different metabolisms. It also requires the consideration of a variety of substrates, including organic carbons and oxygen. The model assumes that the microorganisms responsible for biodegradation can be roughly divided into two functional bacterial groups (oxidizing bacteria for Fe^{2+} and As(III)) in the immobile bio phase. The bacteria group XO_1 uses molecular oxygen to oxidize organic carbon and utilize Fe^{2+} as an electron donor while bacteria XO_2 uses As(III) as electron donor for metabolism to make Fe^{3+} and As(V), respectively. Based on the bacterial activity microbially mediated redox processes are described by the following reactions [23];

Iron Oxidation (XO_1);

$$2CH_2O + 4Fe^{2+} + 3O_2 + 10H_2O \rightarrow 2HCO_3^- + 4Fe(OH)_3 + 10H^+ \quad (1)$$

Arsenic (H_3AsO_3)-Oxidation (XO_2);

$$CH_2O + H_3AsO_3 + 3/2\ O_2 \rightarrow 2HCO_3^- + H_2AsO_4^- + 2H^+ \quad (2)$$

Adsorption of As(V) on Iron-Oxide

$$Fe(OH)_3 + H_2AsO_4^- \rightarrow Fe(OH)_3.H_2AsO_4^- \quad (3)$$

Fe^{2+} is oxidized by dissolves oxygen present in the water. The rate of oxidation of Fe^{2+} is large where both Fe^{2+} and DO are high. Precipitation of Fe^{2+} by oxidation results in the increase of oxi-iron hydroxide which is simply denoted by $Fe(OH)_3$. The oxidation reaction disregarding bacteria mediated oxidation is written as:

$$4Fe^{2+} + O_2 + 8OH^- + 2H_2O \leftrightarrow \quad 4Fe(OH)_3 \quad (4)$$

where O_2 corresponds to DO. Equation (4) represents that 1 mol L^{-1} of Fe^{2+} and (1/4) mol L^{-1} of oxygen O_2 are consumed to precipitate 1 mol L^{-1} of $Fe(OH)_3$. The coefficient (1/4) of the last term in Equation (26) corresponds to the stoichiometric relation in Equation (6). The rate of the precipitation of $Fe(OH)_3$ can be expressed by [22-24]:

$$S_{Fe} = K_{Fe}[Fe^{2+}][OH^-]^2 P_{O2} \quad (5)$$

where S_{Fe} is the rate of precipitation in mol L^{-1} s^{-1}, K_{Fe} is the reaction rate coefficient in atm^{-1} s^{-1}. $[Fe^{2+}]$ is the concentration of Fe^{2+} in mol L^{-1}, $[OH^-]$ is the hydroxide concentration in mol L^{-1}, and P_{O2} is the oxygen partition pressure in atm.

Similarly, based on the Equation (3) the rate of the adsorption/co-precipitation of As(V) with $Fe(OH)_3$ can be expressed by the following equation:

$$S_{Fe\text{-}As} = K_{Fe\text{-}As}[Fe(OH)_3][\ H_2AsO_4^-] \quad (6)$$

where $S_{Fe\text{-}As}$ is the rate of adsorption/co-precipitation in mol L^{-1} s^{-1}, $K_{Fe\text{-}As}$ is the reaction rate coefficient in atm^{-1} s^{-1} for Fe-As. $[Fe(OH)_3]$ is the concentration of $Fe(OH)_3$ in mol L^{-1}, $[H_2AsO_4^-]$ is the As(V) concentration in mol L^{-1} respectively.

2.3 Bacteria growth

The bacteria uses dissolved organic carbon, chemically defined as CH_2O, and the utilizable portion of dead bacteria of 90% as their substrate [24-27]. In the model, the source of organic carbon is the dissolved organic carbon available in the mobile phase. However, bacteria growth is often

controlled by availability of substrates. The growth of bacteria is generally described by the Double Monod kinetic equation [24-26] and can be written as follows:

$$\frac{\partial X}{\partial t} = \nu_{\max} \cdot \frac{C_1}{K_{s1} + C_1} \cdot \frac{C_2}{K_{s2} + C_2} \cdot X \tag{7}$$

where $\nu_{\max}$ is the maximum growth rate, C_1 is the primary substrate (electron donor) concentration in bio phase, C_2 is the secondary substrate (electron acceptor) concentration in bio phase, K_{s1} is the primary substrate half-saturation constant, K_{s2} is the secondary substrate half-saturation constant, and X is the bacteria concentration. If the concentrations of all relevant substrates (usually organic carbon and electron acceptors) in the bio phase are high, microorganisms grow exponentially according to the maximum growth rate ν_{max}.

The net growth of bacterial population is the difference between the growth and decay. The decay of bacteria population is described by the first order rate equation can be written as:

$$\frac{\partial X}{\partial t} = -\nu_{dec} \cdot X \tag{8}$$

where ν_{dec} is the bacteria decay coefficient.

Microbial growth is accompanied by consumption of substrates. The change of CH_2O concentration in the bio phase is linked to the bacteria growth and the consumption of the organic carbon. For the simplified case of only one bacteria group the total change of organic carbon in the bio phase can be expressed by:

$$\frac{\partial [CH_2O]_{bio}}{\partial t} = -\frac{1}{Y_{OC}}\left[\frac{\partial X}{\partial t}\right]_{growth} - f_{use}\left[\frac{\partial X}{\partial t}\right]_{decay} - \frac{\alpha\theta_w}{\theta_{bio} + \theta_w}\left([CH_2O]_{bio} - [CH_2O]_{mob}\right) \tag{9}$$

where the yield coefficient Y_{OC} links microbial growth to organic carbon incorporated into cell mass in a given time interval to the total organic carbon consumption [25]. It is defined as the ratio of organic carbon incorporated into cell mass in a given time interval to the total organic carbon consumption. A part of the organic carbon stored in decaying microbial mass can be reused by the microorganisms. In the model this is simulated by defining an utilizable portion of dead bacteria f_{use}.

The consumption of electron acceptors (e.g. O_2) is correlated to the organic carbon oxidized for energy gain via stoichiometric relations. The concentration change of a mobile electron acceptor in the bio phase is:

$$\frac{\partial [EA]_{bio}}{\partial t} = -\frac{1}{U_{EA}}\left[\frac{\partial X_1}{\partial t}\right]_{growth} - \frac{\alpha\theta_w}{\theta_{bio} + \theta_w}\left([EA]_{bio} - [EA]_{mob}\right) \tag{10}$$

$$U_{EA} = Utilization\ factor = ST.\frac{Y_{OC}}{(1 - Y_{OC})} \tag{11}$$

where ST is the stoichiometric coefficient (e.g. ST for Fe(II) and As(III) are ¼ and ½ respectively) between organic carbon and electron accepter (OC/EA) of the reaction and α is the exchange coefficient to represent the mass transfer between bio and mobile phases through their boundary film.U_{EA} is the utilization factor, Θ_w and Θ_{bio} are the volumetric fraction of water content for the mobile phase and volumetric fraction of bio phase of soil respectively.

Microbial growth does not only cause the consumption of substrates, but also release its metabolic products. The release of metabolic product is related to microbial growth via a production factor P. The production factor for a given metabolic product is stoichiometrically related to the

consumption of an electron acceptor. Thus, the release of the iron- hydroxides is related to bacteria growth:

$$\frac{\partial[H_2AsO_4^-]_{bio}}{\partial t} = \frac{1}{P_{H_2AsO_4^-}}\left[\frac{\partial XO_2}{\partial t}\right]_{growth} - \frac{\alpha\theta_w}{\theta_{bio}+\theta_w}\left([H_2AsO_4^-]_{bio} - [H_2AsO_4^-]_{mob}\right) \quad (12)$$

$$P_{H_2AsO_4^-} = \frac{1}{2}\cdot\frac{Y_{OC}^{H_2AsO_4^-}}{(1-Y_{OC}^{H_2AsO_4^-})} \quad (13)$$

where $P_{H_2AsO_4^-}$ is the production factor for As(V) and $Y_{OC}^{H_2AsO_4^-}$ is the yielding coefficient of As(V).

Based on Monod kinetics, the following mathematical equations are formulated for the growth of two groups of bacteria.

Bacteria XO_1:

$$\left[\frac{\partial XO_1}{\partial t}\right]_{Total\_growth} = \left[\frac{\partial XO_1}{\partial t}\right]_{growth} + \left[\frac{\partial XO_1}{\partial t}\right]_{decay} \quad (14)$$

$$\left[\frac{\partial XO_1}{\partial t}\right]_{growth} = \nu_{\max}^{Fe^{2+}}\cdot\frac{[CH_2O]_{bio}}{K_{CH_2O}+[CH_2O]_{bio}}\cdot\frac{[Fe^{2+}]_{bio}}{K_{Fe^{2+}}+[Fe^{2+}]_{bio}}\cdot XO_1 \quad (15)$$

$$\left[\frac{\partial XO_1}{\partial t}\right]_{decay} = -\nu_{XO_1\,dec}\cdot XO_1 \quad (16)$$

Similarly, same expressions are used to model the Fe^{2+} and As(III) oxidizing bacteria as follows;

Bacteria XO_2:

$$\left[\frac{\partial XO_2}{\partial t}\right]_{Total\_growth} = \left[\frac{\partial XO_2}{\partial t}\right]_{growth} + \left[\frac{\partial XO_2}{\partial t}\right]_{decay} \quad (17)$$

$$\left[\frac{\partial XO_2}{\partial t}\right]_{growth} = \nu_{\max}^{H_3AsO_3}\cdot\frac{[CH_2O]_{bio}}{K_{CH_2O}+[CH_2O]_{bio}}\cdot\frac{[H_2AsO_3]_{bio}}{K_{H_3AsO_3}+[H_2AsO_3]_{bio}}\cdot XO_2 \quad (18)$$

$$\left[\frac{\partial XO_2}{\partial t}\right]_{decay} = -\nu_{XO_2\,dec}\cdot XO_2 \quad (19)$$

2.4 Model equations in mobile, bio and matrix phases

The chemical part of the model incorporates all chemical and biochemical reactions for the chemical species that are considered as shown in **Table 1**. The equations are constructed by mass balances in each phase. In principle all chemical process are time dependent.

Table 1 Chemical species considered in the model.

Mobile phase	$H_2AsO_4^-$, H_3AsO_3, Fe^{2+}, O_2, CH_2O
Bio Phase	Fe^{2+}, $Fe(OH)_3$, O_2, CH_2O, $H_2AsO_4^-$, H_3AsO_3
Bacteria	XO_1 and XO_2
Matrix phase	Fe $(OH)_3$, Fe-As

The model considered the concentration changes of the species in three different phases. The concentration change in mobile phase includes advection, dispersion, mass transfer between mobile and bio phases due to chemical and biochemical processes, and mass transfer between the mobile and matrix phases due to chemical processes. The concentration change in bio phase is result of oxidation reaction by the bacteria growth which is mentioned previously, mass transfer between mobile and bio phases, and mass transfer between bio and matrix phases. The concentration change in matrix phase is result of mass transfer between the bio and matrix phases, and mass transfer between the mobile and matrix phases. **Figure 3** shows the conceptual model of aquifer phases, exchange relation, chemical and biochemical processes of different species residing in the phases.

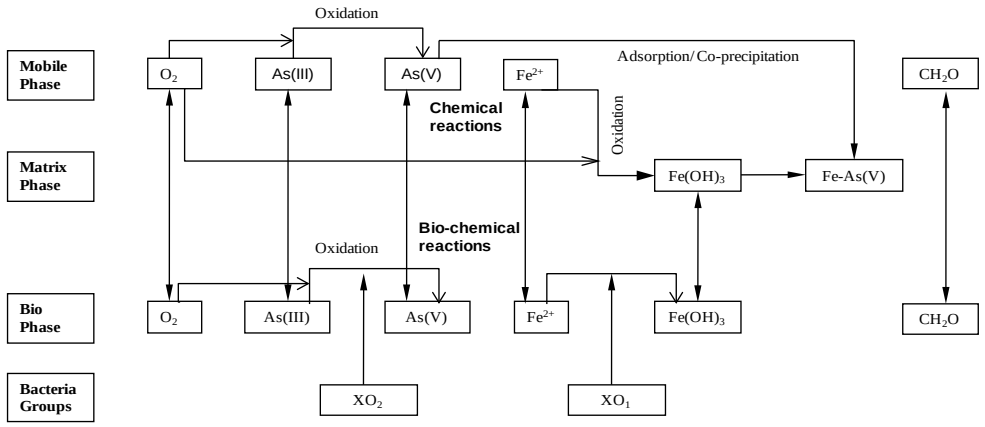

Fig. 3 Conceptual model of the biochemical processes of different species residing in the phases.

Based on the model processes, transport of species in mobile phase can be written as:

Mobile phase; Equation of advection, dispersion with chemical reaction term;

O_2:

$$\frac{\partial [O_2]_{mob}}{\partial t} + \bar{v}\frac{\partial [O_2]_{mob}}{\partial x} = D_L \frac{\partial^2 [O_2]_{mob}}{\partial x^2} + \frac{\alpha\theta_{bio}}{\theta_{bio}+\theta_w}\left([O_2]_{bio} - [O_2]_{mob}\right) - \frac{1}{4}S_{Fe} \tag{20}$$

Fe^{2+}:

$$\frac{\partial [Fe^{2+}]_{mob}}{\partial t} + \bar{v}\frac{\partial [Fe^{2+}]_{mob}}{\partial y} = D_L \frac{\partial^2 [Fe^{2+}]_{mob}}{\partial y^2} - S_{Fe} + \frac{\alpha\theta_{bio}}{\theta_w+\theta_{bio}}\left([Fe^{2+}]_{bio} - [Fe^{2+}]_{mob}\right) \tag{21}$$

CH_2O:

$$\frac{\partial [CH_2O]_{mob}}{\partial t} + \bar{v}\frac{\partial [CH_2O]_{mob}}{\partial y} = D_L \frac{\partial^2 [CH_2O]_{mob}}{\partial y^2} + \frac{\alpha\theta_{bio}}{\theta_w+\theta_{bio}}\left([CH_2O]_{bio} - [CH_2O]_{mob}\right) \tag{22}$$

H_3AsO_3:

$$\frac{\partial [H_3AsO_3]_{mob}}{\partial t} + \bar{v}\frac{\partial [H_3AsO_3]_{mob}}{\partial y} = D_L \frac{\partial^2 [H_3AsO_3]_{mob}}{\partial y^2} + \frac{\alpha\theta_{bio}}{\theta_w+\theta_{bio}}\left([H_3AsO_3]_{bio} - [H_3AsO_3]_{mob}\right) \tag{23}$$

$H_2AsO_4^-$:

$$\frac{\partial[H_2AsO_4^-]_{mob}}{\partial t}+\bar{v}\frac{\partial[H_2AsO_4^-]_{mob}}{\partial y}=D_L\frac{\partial^2[H_2AsO_4^-]_{mob}}{\partial y^2}-S_{Fe-As}+\frac{\alpha\theta_{bio}}{\theta_w+\theta_{bio}}\left([H_2AsO_4^-]_{bio}-[H_2AsO_4^-]_{mob}\right) \quad (24)$$

where β is the exchange coefficient to represent the mass transfer between matrix and mobile phases through their boundary film.

Bio phase;

O_2:

$$\frac{\partial[O_2]_{bio}}{\partial t}=-\frac{1}{U_{O_2}}\left[\frac{\partial XO_1}{\partial t}\right]_{growth}-\frac{1}{U_{O_2}}\left[\frac{\partial XO_2}{\partial t}\right]_{growth}-\frac{\alpha\theta_w}{\theta_{bio}+\theta_w}\left([O_2]_{bio}-[O_2]_{mob}\right) \quad (25)$$

Fe^{2+}:

$$\frac{\partial[Fe^{2+}]_{bio}}{\partial t}=-\frac{1}{U_{Fe^{2+}}}\left[\frac{\partial XO_1}{\partial t}\right]_{growth}-\frac{\alpha\theta_w}{\theta_{bio}+\theta_w}\left([Fe^{2+}]_{bio}-[Fe^{2+}]_{mob}\right) \quad (26)$$

$Fe(OH)_3$:

$$\frac{\partial[Fe(OH)_3]_{bio}}{\partial t}=\frac{1}{P_{Fe(OH)_3}}\left[\frac{\partial XO_1}{\partial t}\right]_{growth}-\frac{\gamma\theta_{mat}}{\theta_{bio}+\theta_{mat}}\left([Fe(OH)_3]_{bio}-[Fe(OH)_3]_{mat}\right) \quad (27)$$

H_3AsO_3:

$$\frac{\partial[H_3AsO_3]_{bio}}{\partial t}=-\frac{1}{U_{H_3AsO_3}}\left[\frac{\partial XO_2}{\partial t}\right]_{growth}-\frac{\alpha\theta_w}{\theta_{bio}+\theta_w}\left([H_3AsO_3]_{bio}-[H_3AsO_3]_{mob}\right) \quad (28)$$

$H_2AsO_4^-$:

$$\frac{\partial[H_2AsO_4^-]_{bio}}{\partial t}=\frac{1}{P_{H_2AsO_4^-}}\left[\frac{\partial XO_2}{\partial t}\right]_{growth}-\frac{\alpha\theta_w}{\theta_{bio}+\theta_w}\left([H_2AsO_4^-]_{bio}-[H_2AsO_4^-]_{mob}\right) \quad (29)$$

CH_2O:

$$\frac{\partial[CH_2O]_{bio}}{\partial t}=-\frac{1}{Y_{CH_2O}^{Fe^{(2+)}}}\left[\frac{\partial XO_1}{\partial t}\right]_{growth}-\frac{1}{Y_{CH_2O}^{H_3AsO_3}}\left[\frac{\partial XO_2}{\partial t}\right]_{growth}+\sum_{i=1}^{2}f_{use}\cdot v_{decay}\cdot X_i-\frac{\alpha\theta_w}{\theta_{bio}+\theta_w}\left([CH_2O]_{bio}-[CH_2O]_{mob.}\right) \quad (30)$$

where γ is the exchange coefficient to represent the mass transfer between bio and matrix phases through their boundary film.

Matrix phase;

$Fe(OH)_3$:

$$\frac{\partial[Fe(OH)_3]_{mat}}{\partial t}=S_{Fe}-S_{Fe-As}+\frac{\gamma\theta_{bio}}{\theta_{bio}+\theta_{mat}}\left([Fe(OH)_3]_{bio}-[Fe(OH)]_{mat}\right) \quad (31)$$

$Fe(H_2AsO_4^-)(OH)_3$:

$$\frac{\partial[Fe(H_2AsO_4^-)(OH)_3]_{mat}}{\partial t}=S_{Fe-As} \quad (32)$$

2.5 Algorithm of numerical simulation and calculation condition

In this model, the whole equation system describing transport, biochemical reactions, chemical equilibrium and chemical kinetics reactions are solved simultaneously. The method of characteristics and the finite difference schemes have been used as numerical solution techniques to solve the model equations[28].

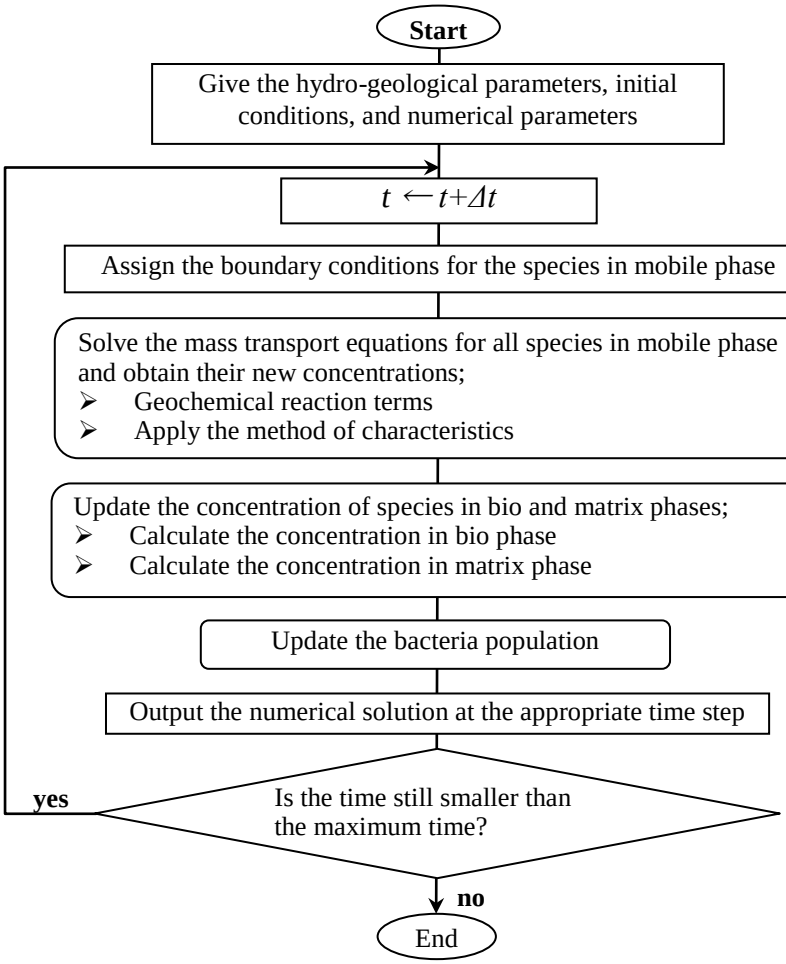

Fig. 4 Illustration of the flow chart for simulating the arsenic transport in groundwater.

A sequential procedure is used where first the advection and dispersion transport equations are solved explicitly for each chemical species. The source /sink terms accounting for reactions are taken from the preceding time step. Then the chemical and biochemical reaction equations are solved with the concentration changes from the transport step as explicit source/sink terms. The exchange processes between the different model phases are also calculated in the biochemical reaction step. The general procedures performed in model for a typical simulation is shown in **Fig. 4**.

The model of solute transport with bioremediation processes is highly complex, as it involves a large number of parameters. The biochemical parameters, and exchange parameters used in this model are displayed in **Table 2**. Monod kinetic, stoichiometric and switching function parameters were taken from several studies related to biochemical simulation [25-26]. The yield coefficients of the different bacterial groups were chosen according to the energy gain of the mediated redox reaction [26]. Decay of bacteria is simulated by a constant decay rate. The decay rate was set to 10% of the maximum growth rate. The initial conditions were selected as zero for all chemical species and boundary conditions were selected depending on the data available in literature [27]. The discretization and hydraulic parameters are presented in **Table 2**. The discretization is selected such that it meets numerical stability and accuracy criteria [Courant number = $(v\Delta t)/\ \Delta x \leq 1$ and grid-Peclet number = $\Delta x\ /\alpha_L \leq 2$]. The pore water velocity of the column was calculated by Darcy's Law.

Table 2 Parameters used for the simulation.

	Biochemical parameter	Parameter values
Exchange coefficient	Bio-Mobile: α	10 day^{-1}
	Bio-Matrix: β	0.005day^{-1}
	Matrix-Mobile: γ	0.00005day^{-1}
Monod half velocity	K_{CH_2O}	0. 1 mmol L^{-1}
	K_{O_2}, $K_{H_2AsO_4^-}$, $K_{Fe(OH)_3}$, K_{Fe-As}	0.001 mmol L^{-1}
Fe(II) Oxidizing bacteria XO_1	Yield Coefficient $Y_{CH_2O}^{Fe^{2+}}$	0.6 mol cell-C/mol OC
	Maximum growth rate $\nu_{\max}^{Fe^{2+}}$	0.02day^{-1}
	Constant decay rate $\nu_{XO_1 dec}$	0.002 day^{-1}
As(III) oxidizing bacteria XO_2	Yield Coefficient $Y_{CH_2O}^{H_3AsO_3}$	0.75 mol cell-C/mol OC
	Maximum growth rate $\nu_{\max}^{H_3AsO_3}$	0.2 day^{-1}
	Constant decay rate $\nu_{XO_2 dec}$	0.02 day^{-1}
Reaction rate coefficients	For Iron hydroxide K_{Fe}	$1.5x10^5$ atm^{-1} s^{-1}
	For Fe-As $K_{Fe\text{-}As}$	$1.5x10^{-6}$ atm^{-1} s^{-1}
Specific volume	Mobile phase: θ_w	0.3
	Bio phase: θ_{bio}	0.02
	Matrix phase: θ_{mat}	0.68

Table 3 Calculation conditions.

Calculation depth L	30 cm
Column diameter	10 cm
Calculation period	30 days
Grid mesh size Δy	0.6 cm
Time increment Δt	10 s
Pore water velocity v	0.00001 cms^{-1}
Porosity n	0.3
Longitudinal dispersion length α_L	0.02 cm
Molecular diffusion coefficient D_M	1.0×10^{-5} cm^2s^{-1}
Gas constant	0.082
Henry`s constant H	30.05
Hydroxyl ion concentration P_{OH}	7.00
Temperature T	21^0C

3. Simulation Results and Discussion

Figures 5(a) and **5(b)** show the results of simulated bacteria growth with depth. As the model considers calculation length (e.g. 30 cm column) is 30 cm so the upper part of the column contain favorable environment for bacteria growth due to availability of substrate like organic carbon. The growth of bacteria throughout the length is dominated by bacterial group XO_1 (iron(II) oxidizer), which possibly is due to the effect of high concentration of iron(II) with limited organic carbon and available oxygen concentration, followed by bacterial group XO_2 (Arsenic(III) oxidizer) although their magnitude are still low compared to the bacteria XO_1. The living bacteria population increases rapidly with time at an exponential growth in numbers, and the growth rate increasing with time. After that with the exhaustion of nutrients and secondary metabolic products, the growth rate has slowed to the point where the growth rate equals the death rate.

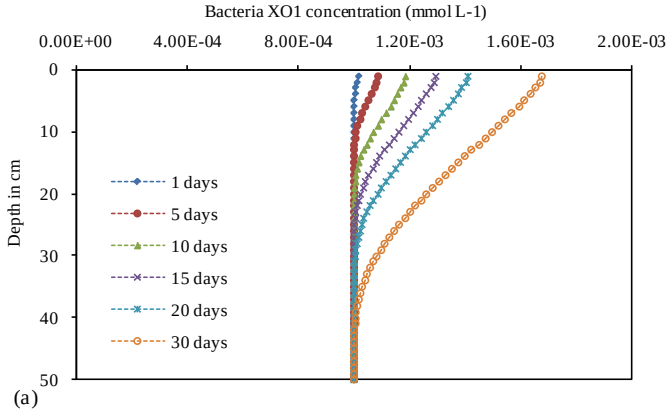
Bacteria XO1 concentration (mmol L-1)
0.00E+00
4.00E-04
8.00E-04
1.20E-03
1.60E-03
2.00E-03
Depth in cm
0
10
20
30
40
50
1 days
5 days
10 days
15 days
20 days
30 days

(a)

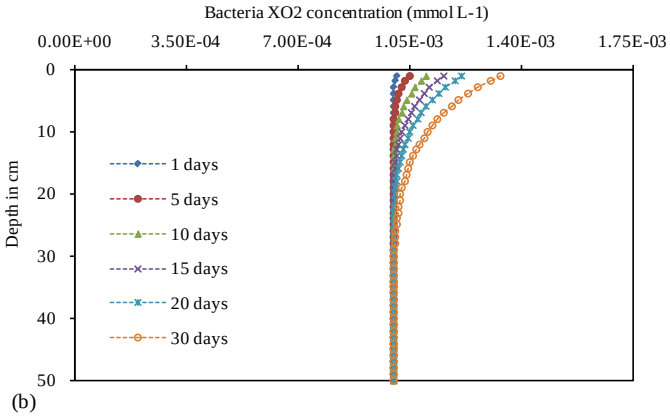
Bacteria XO2 concentration (mmol L-1)
0.00E+00
3.50E-04
7.00E-04
1.05E-03
1.40E-03
1.75E-03
Depth in cm
0
10
20
30
40
50
1 days
5 days
10 days
15 days
20 days
30 days

(b)

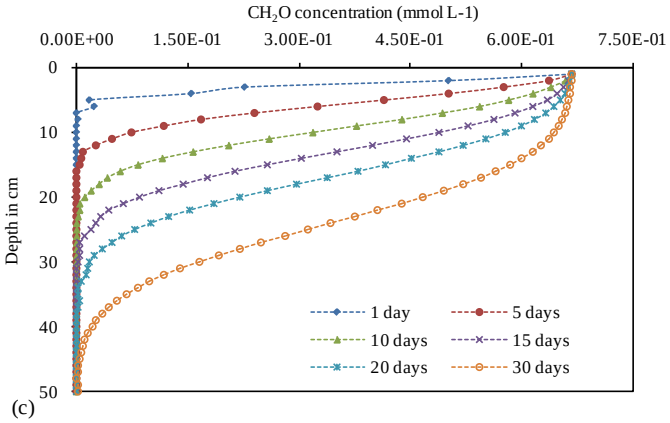
CH2O concentration (mmol L-1)
0.00E+00
1.50E-01
3.00E-01
4.50E-01
6.00E-01
7.50E-01
Depth in cm
0
10
20
30
40
50
1 day
5 days
10 days
15 days
20 days
30 days

(c)

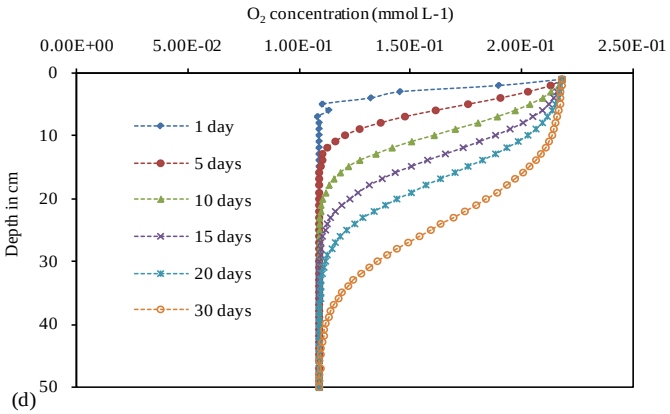

Fig. 5 Simulation results of (a) bacteria XO_1 growth with depth on different days, (b) bacteria XO_2 growth with depth on different days, (c) CH_2O concentrations with depth on different days, (d) O_2 concentrations with depth on different days.

Figures 5(c) and **5(d)** demonstrate the dependence of organic carbon and oxygen distribution with depth at different time in mobile phase. The model simulation results show that the upper part of the calculation length is most important for oxygen, and organic carbon (OC) consumption by micro-organism. Though oxygen and OC are continuously supplied at the inlet of the column, oxygen concentration decreased until OC has consumed to zero by the iron(II) and arsenic(III) oxidizing bacteria XO_1 and XO_2, respectively.

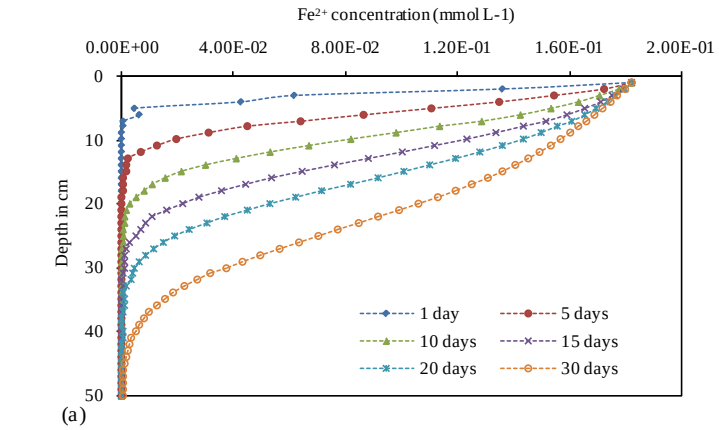

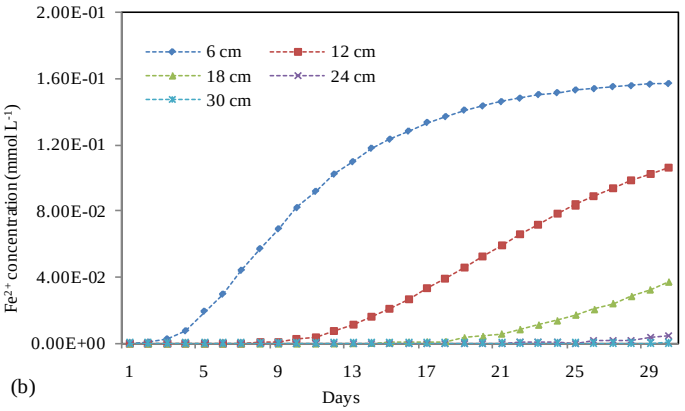

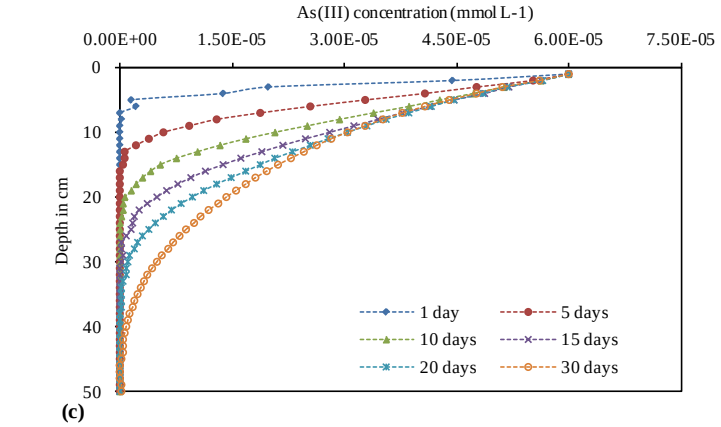
As(III) concentration (mmol L-1)
0.00E+00
1.50E-05
3.00E-05
4.50E-05
6.00E-05
7.50E-05
0
10
20
30
40
50
Depth in cm
1 day
5 days
10 days
15 days
20 days
30 days

(c)

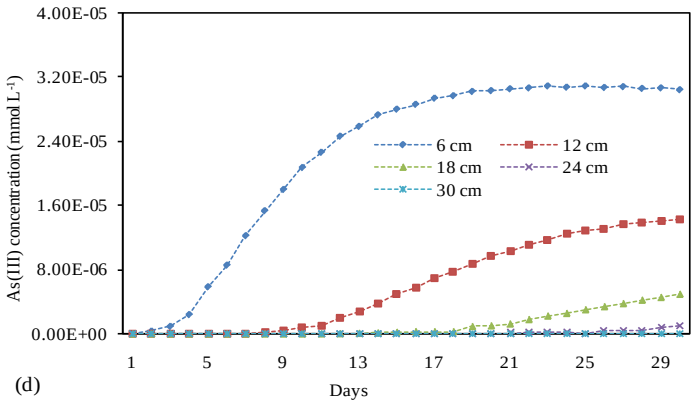
4.00E-05
3.20E-05
2.40E-05
1.60E-05
8.00E-06
0.00E+00
As(III) concentration (mmol L-1)
6 cm
12 cm
18 cm
24 cm
30 cm
1
5
9
13
17
21
25
29
Days

(d)

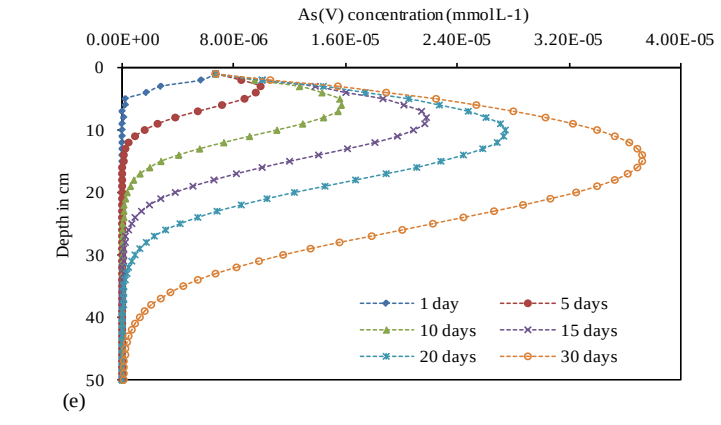
As(V) concentration (mmolL-1)
0.00E+00
8.00E-06
1.60E-05
2.40E-05
3.20E-05
4.00E-05
0
10
20
30
40
50
Depth in cm
1 day
5 days
10 days
15 days
20 days
30 days

(e)

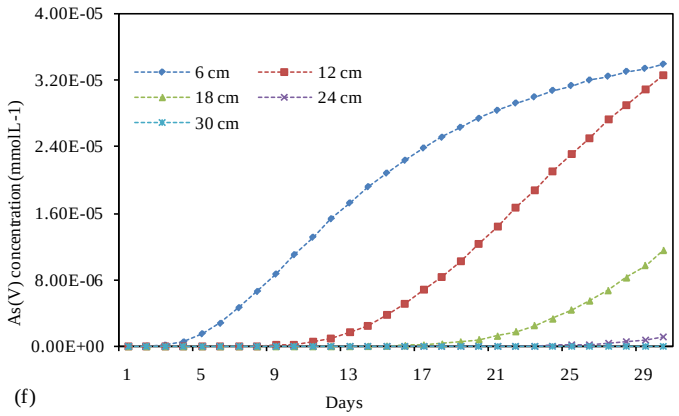
4.00E-05
3.20E-05
2.40E-05
1.60E-05
8.00E-06
0.00E+00
As(V) concentration (mmolL-1)
6 cm
12 cm
18 cm
24 cm
30 cm
1
5
9
13
17
21
25
29
Days

(f)

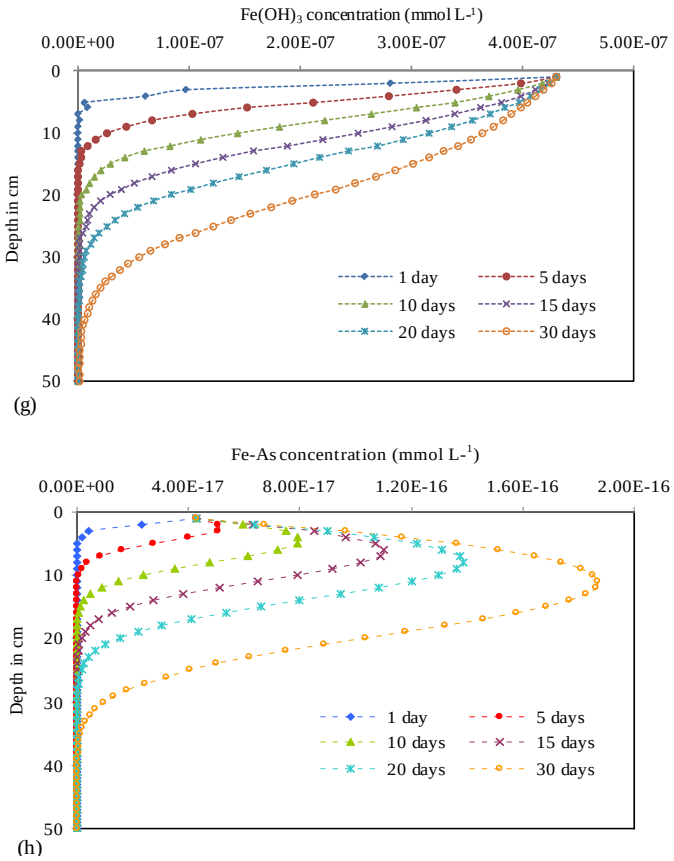

Fig. 6 Simulation results of (a) Fe^{2+} concentration with depth, (b) Fe^{2+} concentration with time at different depths (c) As(III) concentration with depth (d) As(III) concentration with time at different depths (e) As(V) concentration with depth and (f) As(V) concentration with time at different depths(g) $Fe(OH)_3$ concentration with depth and (h) Fe-As concentration with depth.

Figures 6(a) and **6(b)** demonstrate the concentration of Fe^{2+} with depths and with time respectively obtained by numerical simulation. Fe^{2+} concentration decreased due to activity of Fe^{2+} oxidizer (bacteria group XO_1). Bacteria XO_1 uses Fe^{2+} as a electron donor and oxidize it to $Fe(OH)_3$ until organic carbon available in the groundwater for metabolism.

Figures 6(c) and **6(d)** show the concentration of As(III) with depths at different time and with time at different depths. Arsenic (III) concentration start to decrease due to the activity of As(III) oxidizer (bacteria group XO_2). Bacteria group XO_2 oxidize As(III) to As(V) by using organic carbon as substrate for their metabolism. As(V) concentration increase in the upper part of the length by the activity of arsenic(III) oxidizing bacteria simultaneously decreased by adsorption with $Fe(OH)_3$ as shown in **Fig. 6(e)** and **6(f)**. Bacteria growth decreased due to insufficient OC concentration, so the As reduced at to zero.

Figures 6(g) demonstrate concentration of $Fe(OH)_3$ with length on different days. The concentration of Fe-As compound formed by of As(V) adsorption on $Fe(OH)_3$ has also been generated numerically (**Fig. 6(h)**). Initially, Fe-As increase because availability $Fe(OH)_3$ formed by iron oxidizing bacteria and arsenic(V) by arsenic oxidizing bacteria which is due to presence of OC then it decreases to zero.

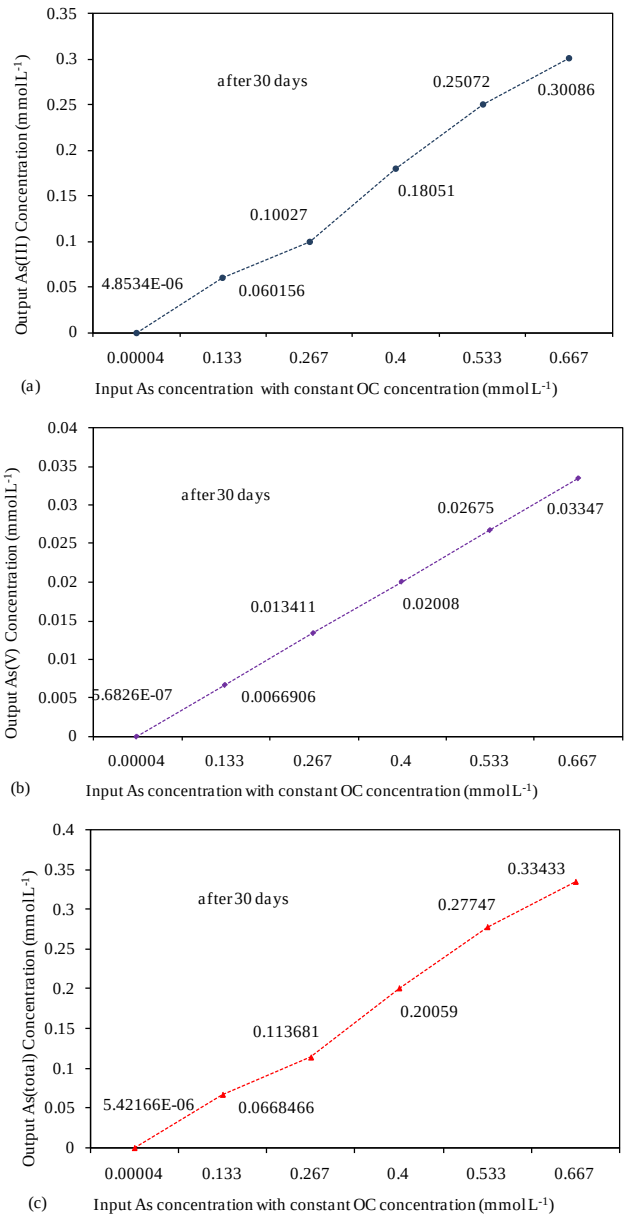

Fig. 7 Simulation results of (a) As(III) concentrations (b) As(V) concentrations and (c) As(total) concentrations, with As variation in input concentration at constant OC concentration.

Figures 7(a), 7(b) and **7(c)** show the output concentration of As(III), As(V) and As(total) after 30 days increase with the increase of arsenic in input concentration at constant organic carbon concentration, respectively. Total arsenic concentration in output increase gradually with increase in input value due to organic carbon concentration. Only 19 ppm OC is provided as input value and it is not sufficient for bacteria metabolism to remove all of the arsenic. Until OC is available in the groundwater oxidizing bacteria can survive to oxidize iron(II) to iron oxide and arsenic(III) to arsenic(V) and form Fe-As compound by adsorption which is led to remove As from groundwater.

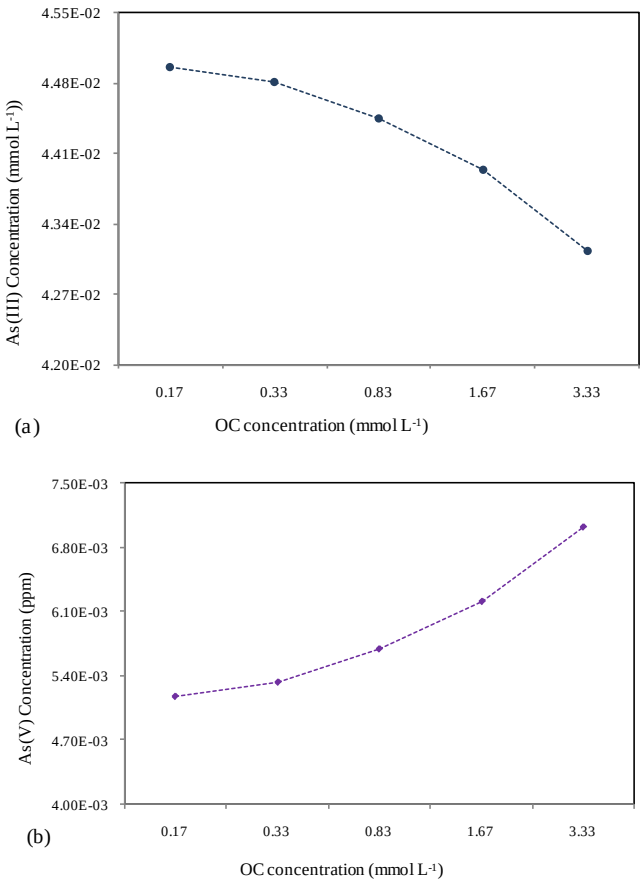

Fig. 8 Effect of OC concentration on (a) As(III) concentrations (b) As(V) concentrations with constant As (1.33 mmol L^{-1})concentration for input value after 30 days.

Figures 8(a) and **8(b)** show the output concentration of As(III) and As(V) after 30 days respectively, with the different organic carbon concentration. In **Fig. 8(a)**, As(III) decreased with increasing organic carbon concentration subsequently in **Fig. 8(b)**, As(V) increase with increase of OC due to the activity of arsenic oxidizing bacteria XO_1. Arsenic oxidizing bacteria uses OC as their substrate for metabolism and oxidize As(III) to As(V). As(V) concentration increased because of the production rate of As(V) is higher than the adsorption rate on the iron oxides.

4. Conclusions

A reactive transport model for describing the microbially mediated transformation of different contaminant and their subsequent removal is developed. In the model, initial arsenic concentration in the water dominated by arsenic(III) concentrations as model considers geochemical features of arsenic contaminated water. Arsenic(III) and Fe(II) oxidizes to As(V) and Fe(III) respectively by oxidizing bacteria and form compounds (Fe-As) by adsorption. Under oxic conditions, arsenite can serve as a terminal electron acceptor in the biological oxidation of organic matter.

The proposed contaminant removal model may serve as a useful tool for predicting the fate and removal of different arsenic species, iron and other species in groundwater systems considering bacteria mediated oxidation chemical and bio-chemical processes. So that the designing of an arsenic removal scheme can be made easily or it could be happen to check different parameter that affect arsenic removal in different scenario. The results of this removal simulation model

demonstrated that availability of substrate (e.g. organic carbon), maximum growth rate, yield coefficient of bacteria, the precipitation rate of iron-hydroxide and the adsorption/precipitation rate of arsenic with iron hydroxide were important parameters which affected the removal of arsenic from groundwater. It was also shown that among all the parameters organic carbon concentration proved as the most important. Furthermore, evaluation of model accuracy will be needed.

Acknowledgements

Ministry of Education, Culture, Sports, Science and Technology, Japan and Mayor, Dhaka city corporation (DCC), Bangladesh are gratefully acknowledged for providing scholarship (Mombukagakusho) to the first author to carry out the research in Japan and allowing first author to conduct the research, respectively.

References

1) Katsoyiannis I. A., Zikoudi, A., Hug, H. J., (2008) Arsenic removal from groundwaters containing iron, ammonium, manganese and phosphate: A case study from a treatment unit in northern Greece. Desalination 224:330-339.
2) WHO (2004) Guideline for drinking water quality, recommendations, vol 1, 3rd edn. World Health Organization, Geneva, p 515
3) BGS and DPHE, (2001). Arsenic contamination of groundwater in Bangladesh. In: Kinniburgh, D.G., Smedley P.L. (Eds.), Volumen 1: Summary. British Geological Survey Report WC/00/19. British Geological Survey, Keyworth.
4) Vaclavikova, M., Gallios, G., P., Hredzak, S., Jakabsky, S., (2008). Removal of arsenic from water streams: an overview of available techniques. Clean T. En. Policy, 10:89–95
5) Shih MC (2005) An overview of arsenic removal by pressure-driven membrane process. Desalination 172:85–97
6) Katsoyiannis I. A. and Zouboulis A. I., (2004) Application of biological processes for the removal of arsenic from groundwaters. Water Res 38:17–26
7) Cullen, W. R.; Reimer, K. J (1989). Arsenic speciation in the environment. *Chem. Rev*. *89*, 713.
8) Shevade S, Ford RG (2004) Use of synthetic zeolite for arsenate removal from pollutant water. Water Res 38:3197–3204
9) Hering JG, Chen PY, Wilke JA, Elimelech M (1997) Arsenic removal from drinking water during coagulation. J Environ Eng 8:800–807
10) Song S, Lopez-Valdivieso A, Hermandez-Campos DJ, Peng C, Monroy-Fermandez MG, Razo-Soto I (2006), Arsenic removal from high arsenic water by enhanced coagulation with ferric ions and coarse calcite. Water Res 40:364–372
11) Ning R. Y., (2002). Arsenic removal by reverse osmosis. Desalination 143:237–241
12) Shih MC (2005) An overview of arsenic removal by pressure-driven membrane process. Desalination 172:85–97
13) Kundu S, Gupta AK (2005) Analysis and modeling of fixed bed column operations on As(V) removal by adsorption onto iron oxide-coated cement (IOCC). J Colloid Interface Sci 290:52–60
14) Dutta A, Chaudhuri M (1991) Removal of arsenic from ground water by lime softening with powdered coal additive. J Water SRT-Aqua 40:25–29
15) Katsoyiannis I. A., Zouboulis A. I., Jekel, M., (2004). Kinetics of Bacterial As(III) Oxidation and Subsequent As(V) Removal by Sorption onto Biogenic Manganese Oxides during Groundwater Treatment. *Ind. Eng. Chem. Res; 43*, 486-493
16) Jekel M. R. (1994). Removal of arsenic in drinking water treatment. In: Nriagu J. O., editor. Arsenic in the environment: part I: Cycling and characterization. New York. Wiley-Interscience; p. 119– 30
17) Kim, M. J., Nriangu J., (2000). Oxidation of arsenite in groundwater using ozone and oxygen. Sci Total Environ; 247:71– 9.

18) Battaglia-Brunet, F.; Dictro, M.-C.; Garrido, F.; Crouzet, C.; Morin, D.; Dekeyser, K.; Clarens, M.; Baranger, P., (2002). An arsenic-(III) oxidizing bacterial population: Selection, characterization and performance in reactors. *J. Appl. Microbiol*. *93*, 656.
19) Katsoyiannis, I.; Zouboulis, A.; Althoff, H W.; Bartel, H., (2002). As(III) removal from groundwater using fixed bed upflow bioreactors. Chemosphere ; 47, 325
20) Mounchet, P., (1992). From conventional to biological removal of iron and manganese removal in France. J. Am. Water Works Assoc. 84,158-166.
21) Zouboulis, A. I., Katsoyiannis, I. A., (2005). Recent advances in the bioremediation of arsenic-contaminated groundwaters. Envi. Int.; 31, 213– 219.
22) Jennings, A.A., Kirkner, D.J., and Theis, T.L., (1982): Multicomponent equilibrium chemistry in groundwater quality models, Water Resources Research, Vol. 18, pp.1089-1096.
23) Lensing, H.J., Vogt, M., Herrling, B., 1994. Modeling of biologically mediated redox processes in the subsurface. Journal of hyd. 159, 125-143.
24) Jinno, K., Hosokawa, T., Akagi, K., Hiroshiro, Y., Yasumoto, J., (2007).Geochemical processes and their modeling at the fresh and salt water mixing zone. Model CARE 2007 (IAHS redbook), pp 191-96.
25) Schafer, D., Schafer, W. & Kinzelbach, W. (1998a). Simulation of reactive processes related to biodegradation in aquifers. 1. Structure of the three dimensional reactive transport model. Cont. hyd. 31:167-186.
26) Schafer, D., Schafer, W. & Kinzelbach, W. (1998b). Simulation of reactive processes related to biodegradation in aquifers. 2. Model application to a column study on organic carbon degradation. Cont. hyd. 31:187-209
27) Razzak, A., Jinno, K., Hiroshro, Y., Halim, M. A., and Oda, K.,(2008). Transport Model for Sequential Release of Mn, Fe and As Under Anaerobic Soil Water Environment. Memoirs of the Faculty of Engineering, Kyushu University, Vol.68, No.1 pp.43-59.
28) Jinno, K. 2000. Dispersion Process and Saltwater Intrusion in Groundwater. In: K. Sato and Y. Iwasa (Editors): Groundwater Hydraulics. Springer-Verlag Berlin Heidelberg.